Excitons and optical absorption in one-dimensional extended Hubbard models with short- and long-range interactions

F. B. Gallagher and S. Mazumdar
Department of Physics, University of Arizona, Tucson, Arizona 85721
(Received 19 June 1997)

We show that charge excitations within one-dimensional extended Hubbard models in the limit of large on-site Coulomb interaction can be mapped onto pairs of spin reversals from the ferromagnetic Ising-Heisenberg spin Hamiltonian. The exciton in the extended Hubbard models is equivalent to the bound two-magnon state of the spin Hamiltonian. From exact results for the spin Hamiltonian, for the intersite Coulomb interactions limited between nearest neighbors, the lowest optical exciton is separated in energy from the electron-hole continuum only for the intersite interaction larger than half the one-electron bandwidth. The commutation relationship between spin operators allows us to numerically investigate exciton binding energies and optical absorptions from the ground state in the limit of large on-site Coulomb interaction even for cases where analytic results are not available. For intersite Coulomb interaction limited between nearest neighbors, the binding energy of the lowest optical exciton changes very weakly for realistic Peierls bond dimerization, although there is a profound change in the optical absorption. While in the undimerized chain a single optical exciton can occur, two additional excitons that occur above the threshold of the electron-hole continuum become optically visible in the dimerized case. For long-range intersite Coulomb interactions, multiple excitons can occur even for the undimerized chain, and additional exciton states become optically visible upon dimerization. With the $1/r$ form for the intersite Coulomb interaction, our numerical calculations suggest that the formation of at least one optical exciton is unconditional, unlike the case of nearest-neighbor interaction. The binding energy of the lowest optical exciton again depends weakly on the dimerization for long-range interaction. Our theoretical results can explain the occurrence of two charge-transfer absorption bands in half-filled band segregated stack charge transfer solids below the spin-Peierls dimerization temperature. Our results also suggest that the lowest optical state of π-conjugated polymers, in which Coulomb interactions are long ranged, is necessarily an exciton. [S0163-1829(97)00448-7]

I. INTRODUCTION

While early theories of π-conjugated polymers stressed the role of electron-phonon couplings in these quasi-one-dimensional materials,[1] more recent work has focused on the direct Coulomb interactions among the π electrons.[2] One possible consequence of moderate to large electron-electron interactions, relative to the one-electron bandwidth is that the lowest optical absorption is to an exciton. A large body of experimental literature has indicated the exciton behavior of the optical state in the polydiacetylenes[3] (PDA's) and poly-paraphenylenevinylenes (PPV's).[4] The exciton concept has received strong support from the recent demonstration of lasing action in several substituted PPV's.[5–7] Similarly, theoretical interpretations of the nonlinear optical properties of the PDA's make extensive use of the exciton concept.[8–10] Indeed, it has even been suggested[11] that the resonant nonlinear absorption in these materials[11–13] in the high-energy region is a transition from the optical exciton to a biexciton of appropriate symmetry. Some theoretical evidence for stable biexcitons have been presented.[14–19]

In contrast to the π-conjugated polymers, the role of strong Coulomb interactions and the exciton concept are both well established in the half-filled band segregated and mixed-stack charge-transfer solids. The relative strength of the electron-electron interactions in these systems is considerably stronger.[20,21] Very recently, stable multiexcitons have been demonstrated in the mixed-stack charge-transfer solid anthracene-pyromellitic acid anhydride.[22]

The scopes of the theoretical works on the exciton character of the lowest optically accessible state in these systems are limited in nature, due to the true many-body nature of the electron-electron interactions. Broadly speaking, theoretical work has either included the electronic correlations only between molecular orbital configurations that are excited to lowest orders with respect to the noninteracting ground state,[9,23–26] or have investigated short finite chains numerically.[8,10,14,19] Within the first approach, the energy gap to the electron-hole continuum is obtained from the Hartree-Fock solution to the correlation problem, and is thus independent of the strong on-site Coulomb corrrelation (the Hubbard U) that characterizes these systems. This is clearly an incorrect solution.[2] Furthermore, within this approach, the lowest optical state is necessarily an exciton for nonzero bond dimerization, independent of the strength or the range of the intersite Coulomb interactions, which as we discuss here, is not entirely correct. Within the second approach that emphasizes including correlations to all orders and therefore focuses on short chains, the exciton cannot be treated as a quasiparticle with a momentum-dependent energy. The nature and width of the electron-hole continuum within the finite chain calculations[8,10,14,19] are also not clear, although limited understanding of continuum states have been obtained.[8,25] A recent density matrix renormalization group (DMRG) approach[27] has investigated exciton binding energies from numerical calculations for very long chains, but these results are also quite limited, and no information about the electron-hole contiuum is obtained from these calculation. Furthermore, the DMRG approach has found an unusually strong dependence of the exciton binding energy on the

Peierls bond alternation that characterizes linear chains, a result that is difficult to understand within the context of all existing theories.

In the present work, we focus on the limit of strong Hubbard on-site interaction relative to the one-electron bandwidth. However, intersite Coulomb interactions can be arbitrarily small. The model therefore introduces two scales of energy, and although optical excitation is necessarily due to electron correlations, exciton formation is not guaranteed. In what follows, we shall distinguish between the strongly coupled simple Hubbard model (no intersite interaction), and extended Hubbard models with nonzero intersite interactions. We will further distinguish between short-range (specifically, nearest neighbor) intersite interaction, and the extended Hubbard model with truly long-range intersite interactions. The model with long-range interactions is analogous to the chemists' Pariser-Parr-Pople[28] Hamiltonian for π-conjugated systems. Our goal is to obtain fully momentum-dependent energies of the exciton and electron-hole continuum states in long chains in the limit of large on-site Coulomb repulsion, and to calculate the optical absorptions to these states. The excitons within our solutions are then true elementary excitations. The large Hubbard repulsion limit has been of interest since the inception of the Hubbard model, and has been widely studied in the context of itinerant antiferromagnetism. We show later that results directly relevant for segregated-stack charge-transfer solids with half-filled band are obtained within our model. Although the large on-site interaction approximation does not apply to π-conjugated polymers, we believe that our detailed results provide valuable qualitative insights.

For the case of short-range intersite interactions, the model Hamiltonian has been studied before. Optical absorptions within the dimerized Hubbard Hamiltonian and the undimerized short-range extended Hubbard Hamiltonian in the limit of large on-site interaction were studied by Lyo and Gallinar[29] and Lyo.[30] These authors did not investigate the interesting case of the dimerized extended Hubbard model. A much more thorough analysis of the undimerized as well as the dimerized extended Hubbard model with short-range intersite interaction has recently been presented by Gebhard *et al.*[31,32] The models investigated by Gebhard *et al.* were studied more recently by Yu *et al.*,[33] who, surprisingly, obtained very different energies and bandwidths for the exciton and the electron-hole continuum. All of the above approaches[29–33] involve formidable algebra, and essentially involve diagonalization of the Hamiltonian within the basis of the so-called lower and upper Hubbard subbands.[34,35] For nonzero intersite interactions, the diagonalization, and the calculation of the optical absorption in particular, become rather involved. Consequently, even though the methods can in principle be applied to the case of long-range intersite interactions, the actual procedures quickly begin to get complicated with each additional intersite interaction. Furthermore, the space of two particle–two hole states is also of interest for probing biexciton states,[11–19] and now the available techniques should become even more complicated.

We introduce an approach to charge excitations in the strongly coupled one-dimensional extended Hubbard Hamiltonians here that is simple and pictorial, and that gives results directly within the total energy description. Essentially, we are able to show that in the limit of large on-site interaction, charge excitations of extended Hubbard models with nearest-neighbor electron hopping can be mapped exactly to pairs of spin excitations within Ising-Heisenberg *ferro*magnetic spin Hamiltonians. While it has been known for a long time that the spin excitations from the ground state of Hubbard models can be described within the isotropic antiferromagnetic Heisenberg spin Hamiltonian,[36,37] we are unaware of previous work that has pointed out the present mapping. The only requirement for the mapping is that electron hoppings are between nearest neighbors. For the translationally invariant case with nearest-neighbor Coulomb interaction, exact solutions of the spin model then become available. Since spin operators on different sites commute, and since the subspaces containing a few spin reversals is small even for very long chains, numerical approaches to the exciton problem become accessible for the cases where exact solutions are not available. We are thus able to deal with the case of long-range interactions for the first time, albeit numerically. Elsewhere, we will discuss analytical and numerical solutions to the biexciton problem.[38]

In Sec. II we present the transformation from the electron Hamiltonian to the spin Hamiltonian. The case of the nearest-neighbor intersite Coulomb interactions are discussed in Sec. III. Our calculated energies and optical absorption spectra are identical with those obtained by that obtained by Gebhard *et al.*,[31,32] and are to be taken as complementary to the procedure adopted by these authors. The transformation to the spin Hamiltonian leads to physically transparent configuration space solutions, that are particularly useful in understanding the details of the complicated optical absorption spectra of dimerized chains (see below). Our results are in disagreement with those of Yu *et al.*[33] Furthermore, at least in the strong on-site Coulomb interaction limit, we do not find the qualitative difference in exciton binding energies between undimerized and Peierls-dimerized chains found within the DMRG calculation.[27] In Sec. IV, we discuss the case of long-range Coulomb interactions, with a $1/r$ form for the potential. In contrast to the case of the short-range interaction, which can lead to a single optically allowed exciton in the absence of Peierls dimerization, multiple excitons are obtained for the case of long-range Coulomb interaction. The binding energy of the lowest optical exciton again depends only weakly on dimerization. In Sec. V, we summarize our conclusions, and also discuss optical absorption below the spin-Peierls transition temperature in half-filled band-segregated stack charge-transfer solids.

II. FERMION TO SPIN HAMILTONIAN

We will consider the extended Hubbard Hamiltonians,

$$H = U\sum_i n_{i,\uparrow}n_{i,\downarrow} + \sum_{i,j} V_j(n_i-1)(n_{i+j}-1) - \sum_i t_i(c^\dagger_{i,\sigma}c_{i+1,\sigma} + c^\dagger_{i+1,\sigma}c_{i,\sigma}). \quad (1)$$

In the above, $c^\dagger_{i,\sigma}$ creates an electron of spin σ on site i, $n_{i,\sigma}=c^\dagger_{i,\sigma}c_{i,\sigma}$ is the number of electrons of spin σ on site i,

and $n_i=\Sigma_\sigma n_{i,\sigma}$. U is the repulsive Coulomb interaction between two electrons on the same site, V_j the interaction between sites j sites apart, and t_i is the one-electron hopping integral. The effect of the Peierls dimerization is included in t_i, which is of the form $t_i=t+(-1)^i\delta$, where δ is a rigid dimerization parameter. We will consider both short-range intersite Coulomb interaction ($V_j=0$ for $j\geqslant 2$) as well as long-range interaction.

We will focus our attention on the limit of large on-site interaction, $U\gg|t|$. Charge-spin decoupling in one dimension in this limit[36,37] implies that subsets of eigenstates can be classified according to the number of double occupancies $N_2=\Sigma_i n_{i,\uparrow}n_{i,\downarrow}$. The ground state lies in the $N_2=0$ subspace, the lowest excitations from which are $N_2=0$ spin excitations.[36,37] Charge excitations occur across a much higher energy and lie in the $N_2=1$ subspace. The double occupancy and the vacancy in $N_2=1$ configurations can move freely in the limit of zero V_j, leading to the electron-hole continuum. For nonzero V_j a bound state with neighboring double occupancy and vacancy can occur, and this is the exciton within the model. Exciton formation depends on the energetics of the $N_2=1$ subspace, while optical absorption results from coupling between the $N_2=0$ ground state and $N_2=1$ subspaces.

We show in this section that the $N_2=1$ subspace of the extended Hubbard Hamiltonian can be transformed to a *ferromagnetic* Ising-Heisenberg spin Hamiltonian in the sector of two reversed spins. We rewrite Eq. (1), separating out electron hops that do and do not conserve N_2:

$$H_\infty=N_2U+\sum_{i,j}V_j(n_i-1)(n_{i+j}-1)+H_1+H_2+H_3, \quad (2a)$$

$$H_1=-\sum_{i,\sigma}t_i(1-n_{i,-\sigma})(c^\dagger_{i,\sigma}c_{i+1,\sigma}+c^\dagger_{i+1,\sigma}c_{i,\sigma})\times(1-n_{i+1,-\sigma}), \quad (2b)$$

$$H_2=-\sum_{i,\sigma}t_i n_{i,-\sigma}(c^\dagger_{i,\sigma}c_{i+1,\sigma}+c^\dagger_{i+1,\sigma}c_{i,\sigma})n_{i+1,-\sigma}, \quad (2c)$$

$$H_3=-\sum_{i,\sigma}t_i[n_{i,-\sigma}c^\dagger_{i,\sigma}c_{i+1,\sigma}(1-n_{i+1,-\sigma})+n_{i+1,-\sigma}c^\dagger_{i+1,\sigma}c_{i,\sigma}(1-n_{i,-\sigma})+\text{H.c.}]. \quad (2d)$$

In the above, H_1 and H_2 describe the independent hoppings of vacancies and double occupancies, respectively. Both these terms conserve N_2. The two terms in H_3 create additional double occupancies and vacancies.

Only H_3 in Eqs. (2) couple the $N_2=1$ subspace to the $N_2=0$ and $N_2=2$ subspaces. In the $U\gg|t|$ limit, this coupling between the $N_2=1$ and $N_2=0$ and 2 is of the same strength as that between spins in the ground state sector, viz., $t_i^2/(U-V_1)$. Compared to the charge gap, the effect of H_3 is therefore negligible in the $U\gg|t|$ limit, and we ignore H_3 in what follows, as in previous work.[29–33] Any errors due to neglecting H_3 are clearly $O(t_i^2/(U-V_1))$.

We point out an important consequence of this decoupling of the $N_2=1$ from all other subspaces. In the following we refer to the double occupancy as the particle, and the vacancy as the hole. Consider an arbitrary many-electron configuration in the $N_2=1$ subspace of a long *open* chain, with the particle to the left of the hole, and arbitrary particle-hole separation. Repeated applications of H_1 and H_2 to this configuration generate all other configurations in which the particle remains to the left of the hole, but configurations in which the particle is to the right of the hole cannot be generated by applications of H_1 and H_2. The only way to generate the set of configurations with the particle to the right, beginning from a configuration in which the particle is to the left of the hole, is to let the particle and the hole approach each other, generate a virtual intermediate $N_2=0$ configuration, and then recreate the particle to the right. The intermediate $N_2=0$ configuration is forbidden in the $H_3=0$ limit. The set of configurations with the particle to the left of the hole are then completely decoupled from the set with the particle to the right. Thus the $H_3=0$ approximation (which is equivalent to the $U\gg|t|$ approximation) introduces a degeneracy between the even and odd parity exciton, where the parity is with respect to the center of inversion of the open chain. The two excitons should have an energy splitting of $O(2t^2/U-V_1)$, but this is of little consequence here, as linear optical absorption involves only the odd parity exciton. It should be kept in mind, however, that *nonlinear* absorption involves also the even parity exciton. The even parity exciton has been referred to as the mA_g state in the context of optical nonlinearity.[8]

Charge-conjugation symmetry in the half-filled extended Hubbard Hamiltonian implies that the Hamiltonian is invariant to the transformation $c^\dagger_{i,\sigma}\rightarrow(-1)^i c_{i,\sigma}$, $c_{i,\sigma}\rightarrow(-1)^i c^\dagger_{i,\sigma}$. Transforming H_2 this way, we find that the transformed H_2 is identical to the untransformed H_1 in Eq. (2b), indicating that there is no difference between the independent motions of the particle and the hole in the $N_2=1$ subspace. For $H_3=0$, and in the absence of V_j, H_∞ therefore simply describes two noninteracting spinless fermions.[39] This character of the Hamiltonian is independent of whether a particle-hole pair or a hole-hole pair is being considered. The particle-hole character of the two spinless fermions in Eq. (2a) then becomes relevant in a single term, viz., the intersite interaction containing V_j, which as it stands would correspond to a repulsion between two holes, as opposed to an attraction between a particle and a hole. If this repulsion is formally replaced with a hole-hole attraction, one obtains a Hamiltonian with two holes whose energy spectrum is identical to that of the original particle-hole Hamiltonian. The new system corresponds to a chain with N sites, $N-2$ of which are singly occupied. As was shown by Klein and Seitz,[39] charge excitations of such a system with unequal numbers of electrons and sites are described within a spinless fermion Hamiltonian,

$$H_{\text{red}}=U-\sum_{i,j}V_j(n_i-1)(n_{i+j}-1)-\sum_i t_i(a_i^\dagger a_{i+1}+a_{i+1}^\dagger a_i), \quad (3)$$

where the operator $a_i^\dagger$ now creates spinless fermions, and $n_i=0$ or 1 only. We have introduced attractive interactions

between the holes based on the reasoning given above.

The Hamiltonian $H_{\rm red}$ in Eq. (3) can now be transformed via the Jordan-Wigner transformation,

$$S_i^\dagger = \exp\left(i\pi \sum_{j<i} a_j^\dagger a_j \right) a_i^\dagger , \tag{4a}$$

$$S_i^z = (1-n_i) - 1/2 \tag{4b}$$

to the *ferromagnetic* Ising-Heisenberg spin Hamiltonian with $N-2$ spins pointing down, and two reversed spins:

$$H_s = U - \sum_{i,j} V_j (S_i^z + 1/2)(S_{i+j}^z + 1/2)$$

$$- \sum_i t_i (S_i^\dagger S_{i+1}^- + S_{i+1}^\dagger S_i^-). \tag{5}$$

We therefore find that the exciton problem within the extended Hubbard Hamiltonian reduces to that of the bound state of two ferromagnetic magnons. Since spin operators on different sites commute, direct numerical calculations of energy spectra and optical absorption now become feasible for the cases where exact analytic solutions are not available.

We now discuss optical absorption to the $N_2=1$ subspace from the $N_2=0$ ground state. For nearest-neighbor charge transfer, the current operator $\hat{j}$ within the full extended Hubbard Hamiltonian of Eq. (1) is given by[40]

$$\hat{j} = -i \sum_i t_i d_i (c_{i,\sigma}^\dagger c_{i+1,\sigma} - c_{i+1,\sigma}^\dagger c_{i,\sigma}), \tag{6}$$

where we have taken the electronic charge e as 1. In Eq. (6), d_i is the distance between atoms i and $i+1$. Exact numerical calculations of optical absorptions of correlated short chains in the past have shown that the explicit inclusion of bond dimerization in Eq. (6) makes little difference in calculated transition dipole moments:[41] the dominant effect of dimerization on the optical absorption comes from the change in the excited-state wave functions induced by the dimerization. We therefore take all $d_i=1$ for convenience. From the nature of the current operator, optical absorption conserves the rotational symmetry K.[40] The optical conductivity $\sigma(\omega)$ is obtained from[40]

$$\mathrm{Re}[\sigma(\omega)] = (\pi/\omega) \sum_n |\langle g|\hat{j}|n\rangle|^2$$

$$\times [\delta(\omega - E_n + E_g) + \delta(\omega - E_g - E_n)], \tag{7}$$

where Re implies the real part, E_g is the energy of the ground state g, and E_n are energies of excited states n to which g is coupled through the current operator $\hat{j}$, and $\omega = \pm(E_n - E_g)$. The optical sum rule, as well as the relationship between the dipole and the current operators have been discussed by many authors over the years[40] and will not be repeated further. In the following, we will be interested in the reduced dimensionless optical conductivity $\omega\ \mathrm{Re}[\sigma(\omega)]/|t|$, which from Eq. (7) is simply proportional to $|\langle g|\hat{j}|n\rangle|^2$, and which hereafter we denote as $|j_{gn}|^2$. In all our figures below, we plot only $|j_{gn}|^2$ in units of $|t|$, and avoid introducing arbitrary broadening parameters.

We assume that the ground state of the extended Hubbard Hamiltonian in the $U \gg |t|$ limit corresponds to the perfectly antiferromagnetic (AF) state. Operating on the $N_2=0$ AF state of the electron Hamiltonian, the current operator generates a particle-hole pair with equal probability from all neighboring pairs of sites. This is exactly equivalent to the generation of two nearest-neighbor holes within the Hamiltonian $H_{\rm red}$ of Eq. (3), and therefore to the generation of two reversed spins from the ferromagnetic ground state of the the spin Hamiltonian H_s. Within H_s, j_{gn} therefore reduces to $\Sigma_i t_i \langle g|S_i^\dagger S_{i+1}^\dagger|n\rangle$. In the following sections we consider the two extreme cases, viz., intersite interactions limited to nearest neighbors ($V_j=0$ for $j \geqslant 2$), and long range Coulomb interactions, separately.

Gebhard *et al.* have discussed the consequence of choosing a ground state different from the AF ground state on the optical absorption.[32] Specifically, the ground-state wave function in one dimension is not AF for any finite U,[2] and even in the absence of electron-phonon couplings that could lead to a spin-Peierls transition, the wave function consists of nearest-neighbor spin singlets as opposed to the AF long-range order.[2] We discuss this issue further in the Appendix, where we show that at least in the $U \gg |t|$ limit, there is no difference in the optical absorptions from the exact ground state and from the perfect AF configuration. In particular, the exciton binding energy and the width of the electron-hole continuum are independent of the choice of the ground state.

III. SHORT-RANGE INTERSITE INTERACTION

In this section we consider the case where the intersite Coulomb repulsion is limited to nonzero nearest-neighbor interaction. This is the case that has been investigated previously.[27,29–33,42] We consider $\delta=0$ and $\delta\neq 0$ separately.

Case A. $\delta=0$. Since we are interested in the long chain limit, we consider H_s within periodic boundary conditions in what follows. The basis functions of H_s for the translationally invariant $\delta=0$ case are

$$\Psi(K;n) = N^{-1/2} \sum_m \exp(iKm)\Phi(m, m+n), \tag{8}$$

where $\Phi(m,m+n)$ denotes two reversed spins occupying sites m and $(m+n)$, respectively, and K is the center-of-mass momentum. Using the above basis, an exact solution to the energy spectrum of H_s has been obtained by Wortis.[43]

The energy spectrum of the two-magnon continuum states, corresponding to the electron-hole continuum in the fermion model, is given by

$$E_c(K) = U - 2|t|\cos K_1 - 2|t|\cos K_2, \tag{9}$$

where K_1 and K_2 are the wave numbers of the two independent spins, and $K = K_1 + K_2$. Within H_s, the individual $K_i = \pm \pi l/N$, where l is an odd integer. The Paulion nature of the spin operators dictates that $K_1 \neq K_2$. The last condition does not arise naturally when considering electron-hole excitations between lower and upper Hubbard subbands, and has to be incorporated extraneously.[31] In the long chain limit the edge of the electron-hole continuum is therefore at

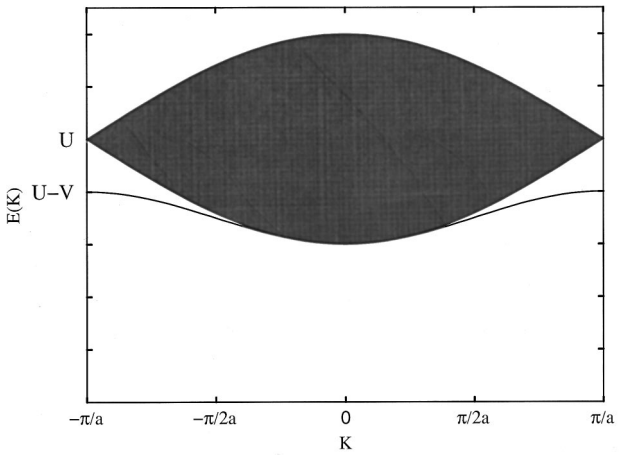

FIG. 1. The energy spectrum of the $N_2=1$ subspace of the undimerized extended Hubbard Hamiltonian with short-range intersite interaction $V_1=2|t|$. Shaded region, electron-hole continuum. The $K=0$ exciton appears only for $V_1>2|t|$.

$U-4|t|$. Our expression for the electron-hole continuum is identical to that obtained by Gebhard *et al.*,[32] and is also in agreement with the exact Bethe ansatz optical gap $U-4t$ within the simple Hubbard model ($V=0$) for large U.[44] Yu *et al.* have determined the energy of the lower threshold of the continuum to be $U-4\delta^2 J$, $J=2t^2/U$. This latter result is clearly in disagreement with the exact solution for the Hubbard Hamiltonian.

In addition to the continuum states, a single bound state of two magnons, corresponding to the exciton within the electron Hamiltonian, occurs for nonzero V_1. The exciton energy $E_{\rm ex}(K)$ is given by[43]

$$E_{\rm ex}(K)=U-V-(4t^2/V_1)\cos^2(K/2). \tag{10}$$

From Eqs. (9) and (10), there is always a bound state at $K=\pi$, but at $K=0$ the bound state appears only for V_1 larger than a critical interaction $V_{1c}=2|t|$. We believe that the present approach involving a transformation to the spin Hamiltonian gives an appealing intuitive understanding of the exciton problem. Once again, our result for the exciton energy dispersion is in agreement with that obtained by Gebhard *et al.*[31] but is in disagreement with that of Yu *et al.*,[33] who find $V_{1c}=2J(1+\delta^2)$. Both the exciton energy dispersion as well as the continuum energy obtained by Yu *et al.* are incorrect.

In Fig. 1 we have shown the energy spectrum of the $N_2=1$ subspace for $V_1=2|t|$. Since the exact wave functions are known,[43] in principle $|j_{gn}|^2$ can be evaluated analytically. However, not only would this approach require evaluations of elliptic integrals at every energy, the procedure does not lead to any new physical insight. Furthermore, for the dimerized extended Hubbard models, evaluations of optical absorptions are necessarily numerical, as in previous work,[31,32] and especially for this case we show that the spin model leads to clear physical interpretations of the different kinds of excitons that are formed. We have therefore calculated $|j_{gn}|^2$ numerically for periodic rings of 100 sites.

Our results for several different cases are plotted in Fig. 2. In Fig. 2(a), $|j_{gn}|^2$ is perfectly symmetric about U, extending from $U-4t$ to $U+4t$. This result agrees with that obtained by Lyo and Gallinar[29] and Gebhard *et al.*[32] for the AF ground state. Very similar absorption was also obtained in an exact numerical calculation for the 12-site periodic ring by Loh and Campbell[42] for the *full* extended Hubbard Hamiltonian of Eq. (1) for $U/|t|=12$, thereby indicating that the $U\gg|t|$ approximation and the transformations above become valid for U as small as $12|t|$. As discussed in the Appendix, the exact optical absorption spectrum for an open chain of 8 atoms with $U=50|t|$ and $V_1=0$ is also similar. Interestingly, the lower edge of the electron-hole continuum continues to be at $U-4|t|$ for even large V_1 ($V_1=15|t|$).[14]

The evolution of the absorption curves in Fig. 2 can be anticipated from the energy dispersion relations [Eqs. (8) and (9)] and Fig. 1. As V_1 increases from zero, the eigenstate that finally evolves as the $K=0$ exciton splits off from the center of the electron-hole continuum at U, and the $|j_{gn}|^2$ curves get progressively skewed towards lower energies as the state shifts towards the bottom of the electron-hole continuum. Note that the edge of the electron-hole continuum continues to be sharply visible in all cases, a result that we will use in Sec. IV for determining the exciton binding energies for the case of long-range V_j. At exactly $V_1=2|t|$ the absorption is most sharply skewed, but the $K=0$ exciton has still not formed. Only for $V_1>2|t|$ a distinct optical transition to the $K=0$ exciton becomes visible. Sum rules[40] dictate that transition to the exciton acquires oscillator strength from the transition to the electron-hole continuum, and with increasing V_1 the oscillator strength of the transition to the continuum band progressively gets weaker.

Case B: $\delta\neq 0$. The absence of translational invariance implies that the $\Psi(K;n)$ in Eq. (8) are no longer proper basis functions, and the approach of Wortis[43] is not applicable. Although approximate closed-form expressions for the energies are still possible, calculations of optical absorption are necessarily numerical even after formidable algebra.[31,32] We choose a different path instead. The commutation properties of the spin operators allow us to simply diagonalize H_s numerically to calculate the exciton binding energies and the optical absorption spectra.

In the absence of V_1, the exact continuum energies $E_c(K)$ can still be obtained:

$$E_c(K)=U-2|t|(\cos^2 K_1+\delta^2\sin^2 K_1)^{1/2} -2|t|(\cos^2 K_2+\delta^2\sin^2 K_2)^{1/2}, \tag{11}$$

where the relationship $K=K_1+K_2$ still applies. As in the case for $\delta=0$,[43] we expect the effect of the exciton state on the continuum states to be still $O(1/N)$. Because of the larger unit cell the Brillouin zone ''folds'' at $K=\pi/2$. Within Eq. (11), the overall width $8|t|$ of the electron-hole continuum remains unchanged upon dimerization, but there is now a gap in the energy spectrum of width $8\delta|t|$ at $K=0$. Furthermore, there is a single $N/2$-fold degenerate exciton state at the center of the gap at energy U, corresponding to all $K_2=K_1+\pi$. Hereafter, we refer to this exciton state, which is formed even in the absence of V_1 as the ''band center'' exciton, to distinguish it from two other excitons that are formed as a consequence of nonzero V_1 (see below).

For $V_1\neq 0$ we obtained the exact energy dispersion curves from the full K-dependent numerical solutions to H_s for a

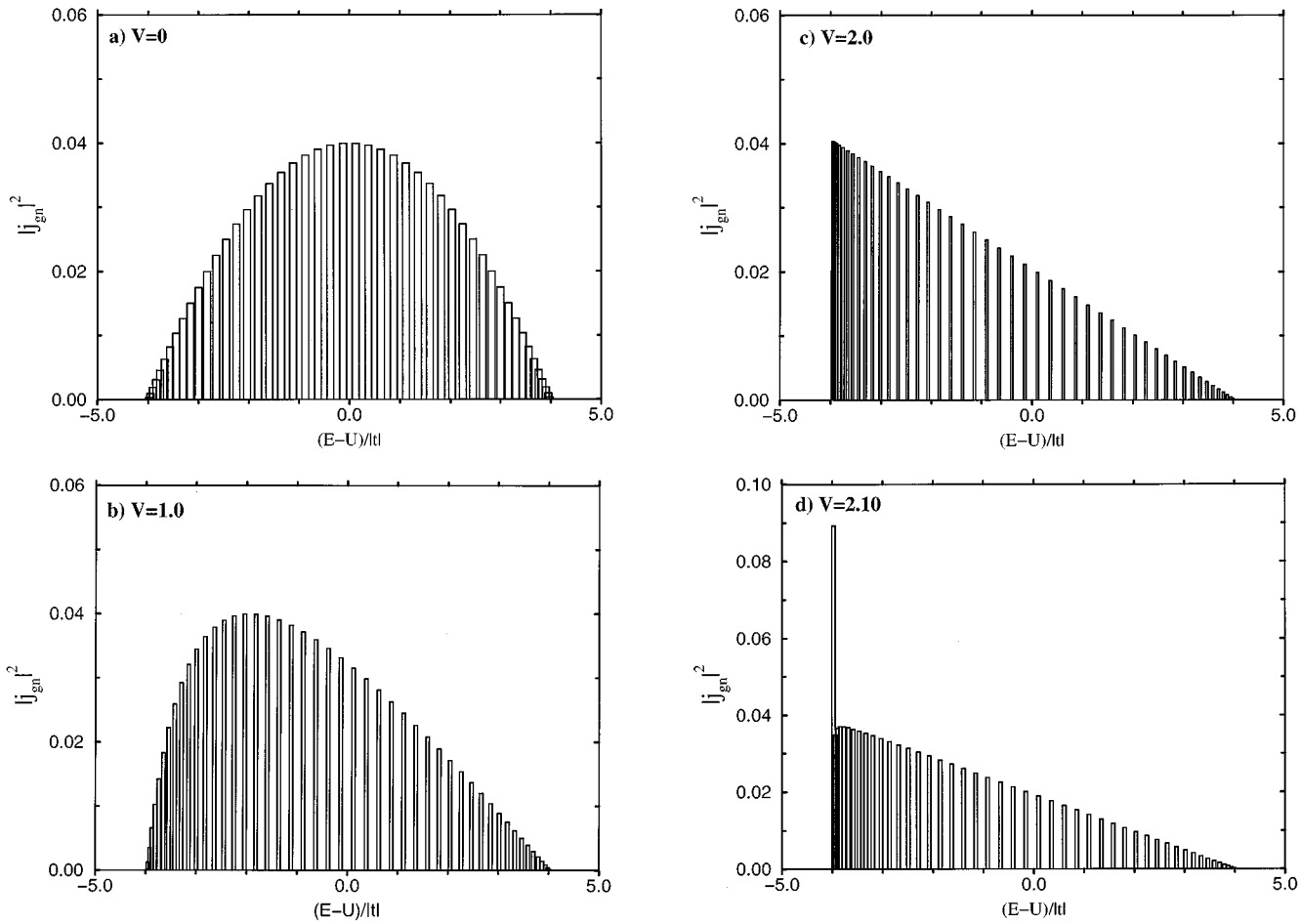

FIG. 2. The reduced optical conductivities for the undimerized extended Hubbard model with short-range intersite interaction, for (a) $V_1=0$, (b) $V_1=|t|$, (c) $V_1=2|t|$, (d) $V_1=2.1|t|$. Each vertical bar corresponds to $|j_{gn}|^2$ for a single excited state n. Only for $V_1>2|t|$ is the $K=0$ exciton split from the electron-hole continuum.

ring of $N=100$. The energy spectrum for the case of $V_1=2|t|$ and $\delta=0.2$ is shown in Fig. 3. As in Fig. 1, the shaded regions correspond to total energy states with delocalized electron-hole pairs, while the individual lines are the exciton states. The dashed line within the energy gap region is the band center exciton that shifts down in energy from U for nonzero V_1. This is due to its interaction with the lowest exciton (see below), whose location is nearly the same as in Fig. 1 for the undimerized extended Hubbard Hamiltonian, with one difference: exactly as the continuum states ''fold'' about $K=\pi/2$, the exciton band of Fig. 1 also ''folds'' about $K=\pi/2$, and the exciton state that was previously at $K=\pi$ and at energy $U-V_1$ is now at $K=0$. Three different $K=0$ exciton states therefore are expected to contribute to optical absorption for $\delta\neq 0$.

We focus first on the binding energy of the lowest exciton, $E_c(K=0)-E_{ex}(K=0)$ as a function of the bond alternation parameter δ. For the case of nearest-neighbor interaction, the binding energy is simply the energy difference between the lowest two eigenstates of H_s, which we evaluated numerically for a periodic ring of 100 sites. In Fig. 4 we have plotted the calculated binding energy of the lowest optical exciton, E_b, as a function of V_1 for several different δ. It is seen that the critical strength of the nearest-neighbor interaction at which the exciton forms, V_{1c}, changes very weakly for moderate δ ($\delta\leqslant 0.3$). E_b for moderate δ are also very close, and as might be anticipated, the relative contribution of dimerization to E_b decreases with increasing V_1. Only for unrealistically large dimerization $\delta\geqslant 0.5$ is there a noticeable effect on V_{1c} and E_b. With further increase in δ, V_{1c} decreases rapidly and reaches the value zero for $\delta=1$.

The exact results for $\delta\neq 0$ in Fig. 4 are in strong disagreement with the DMRG calculation of Shuai *et al.*[27] These authors define the charge gap $E_c(K=0)$, the energy difference between the lower edge of the electron-hole continuum and the ground state, of the N-electron N-site chain as $E(N+1)+E(N-1)-2E(N)$, where the quantities correspond to the ground-state energies of the $N+1$, $N-1$, and N-electron systems (with N sites in all cases), respectively, which are then calculated for long open chains within the DMRG procedure. The exciton binding energy is $E_c(K=0)-E(1B_u)$, where $E(1B_u)$ is the energy of the lowest optical exciton of odd parity B_u symmetry of the N-electron system, and is evaluated using a symmetry-adapted version of the DMRG.[45] Shuai *et al.* evaluate the exciton binding energy for a single U ($U=5|t|$) for several differrent V_1 ($V_1\leqslant 2.3|t|$) for both $\delta=0$ and 0.2, and find that while the binding energy for $\delta=0$ remains practically zero (a result that is in agreement with our conclusion that $V_{1c}=2|t|$), this quantity increases rapidly and abruptly from

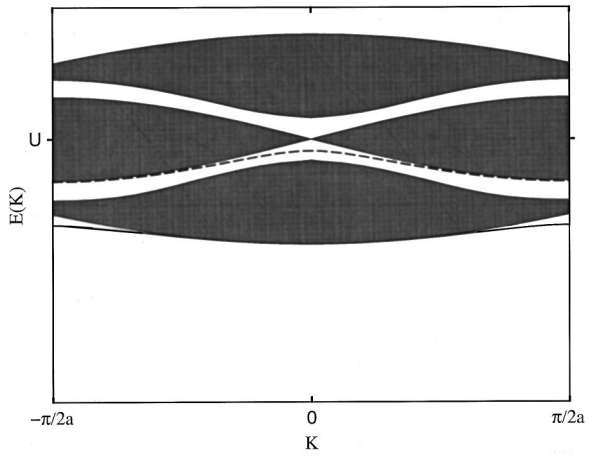

FIG. 3. The energy spectrum of the $N_2=1$ subspace of the dimerized ($\delta=0.2$) extended Hubbard Hamiltonian with short-range intersite interaction $V_1=2|t|$. The shaded region is the electron-hole continuum. The solid line corresponds to the exciton in Fig. 1. A second branch of this occurs inside the electron-hole continuum. The dashed line correponds to the band center exciton that occurs at exactly U for $V_1=0$, and moves down in energy with increasing V_1 (see text).

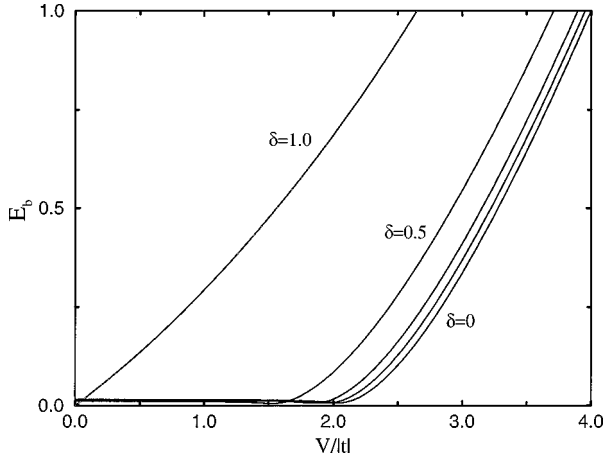

FIG. 4. The binding energy E_b of the lowest $K=0$ exciton, in units of $|t|$, as a function of $V_1/|t|$, for different δ. The two curves bounded by the $\delta=0$ and $\delta=0.5$ correspond to $\delta=0.2$ and 0.3, respectively.

$V_1\simeq|t|$ onwards for $\delta=0.2$. This increase in the binding energy is large enough that at $V_1=2.3|t|$ the binding energy for $\delta=0.2$ is $\sim 0.8|t|$ within the DMRG calculation. Such a *qualitative* difference in the exciton binding energy behavior between $\delta=0$ and $\delta=0.2$ clearly disagrees with the results shown in Fig. 4, where $V_{1c}\sim 1.97|t|$ for $\delta=0.2$ and $V_{1c}\sim 1.6|t|$ even for $\delta=0.5$, and $E_b\leqslant 0.1|t|$ for $V_1=2.5|t|$.

In principle, such a difference could arise from the finite U ($U=5|t|$) in the DMRG calculation and the $U\gg|t|$ limit discussed here. Since, however, the large U approximation to the optical gap[44] already begins to become appropriate for $U>4|t|$,[2] and since the DMRG results for $\delta=0$ (Ref. 27) reproduce our results so well, we suspect that the origin of the discrepancy for $\delta\neq 0$ lies elsewhere. Note that from physical considerations one would anticipate that the exciton binding energy is larger for $U\gg|t|$ than for intermediate U. It is possible that the DMRG procedure loses accuracy for nonzero δ (Shuai *et al.* are able to check against the exact Lieb-Wu $1B_u$ energies for the Hubbard model only for $\delta=0$). It is also possible that Shuai *et al.*'s definition of the charge gap becomes invalid for nonzero δ, given the complex structure of the energy bands for the dimerized lattice in Fig. 3. In any event, the difference between our results and the DMRG calculations is intriguing at the very least, and the origin of the discrepancy can be found out if the DMRG calculations are extended to $U\geqslant 10|t|$, in a region where the results of previous finite-size calculations of optical absorption[42] agree completely with our large U calculations for both $\delta=0$ and $\delta\neq 0$ (see below). A $U\geqslant 10|t|$ will also allow the DMRG procedure to be extended to V_1 considerably larger than $V_{1c}=2|t|$ (Shuai *et al.*'s current limitation to $V_1=2.3|t|$ for $U=5|t|$ arises from the condition $U\geqslant 2V_1$, which defines the boundary between the bond order wave and the site-diagonal charge density wave[46]). DMRG results in the large U range will clearly show whether the discrepancy is due to a fundamental difference between intermediate and large U, or whether there exists an error in the existing DMRG calculations.

As can be anticipated from Fig. 3, profound changes in the optical absorption are expected upon dimerization. In particular, three distinct exciton states are expected to become optically visible for $V_1>V_{1c}$ now. In Fig. 5 we have plotted $|j_{gn}|^2$ for various V_1 and $\delta=0.2$. The results for other δ are qualitatively similar. For $V_1=0$, a strong absorption appears to the band center exciton at U, and the electron-hole continuum is split into two subbands, symmetrically displaced about the central peak. For $V_1<2|t|$ the lowest exciton is still not visible, as in Fig. 2, but the exciton state that occurred at $K=\pi$ for $\delta=0$ and the band center exciton are both visible. The band center exciton has moved down in energy from U, and has also lost oscillator strength due to interaction with the state that finally evolves as the lowest exciton. The latter effect is more clearly visible in Fig. 5(c), where the lowest exciton has already formed (our numerical estimate for $V_{1c}=1.97|t|$ for $\delta=0.2$). As for $\delta=0$, with increasing V_1, the oscillator strength concentrates in the lowest exciton, which now steals oscillator strength largely from the band center exciton that continues to move down in energy. In contrast, the exciton state that was previously at $K=\pi$ continues to occur at $U-V_1$ for all V_1, and has nearly the same oscillator strength.

Since our calculations are within configuration space, we are able to obtain distinct physical interpretations for all the exciton states that become optically accessible for nonzero δ. In Table I, we have described the wave functions for the three exciton states, which are labeled as $K=0$, π, and U, in increasing order of energy. With nearest-neighbor Coulomb interaction, the exciton states have the particle-hole pair (the reversed spins within H_s) localized on neighboring atomic sites. For nonzero δ there occur two kinds of neighboring bonds, and these are labeled as ''short'' and ''long'' in Table I. The numbers against these are the normalized coefficients of the basis functions with the particle-hole pair localized on the two kinds of bonds. The difference between the $K=0$ and $K=\pi$ excitons arise from the relative signs of these coefficients. Surprisingly, the lowest exciton is located pre-

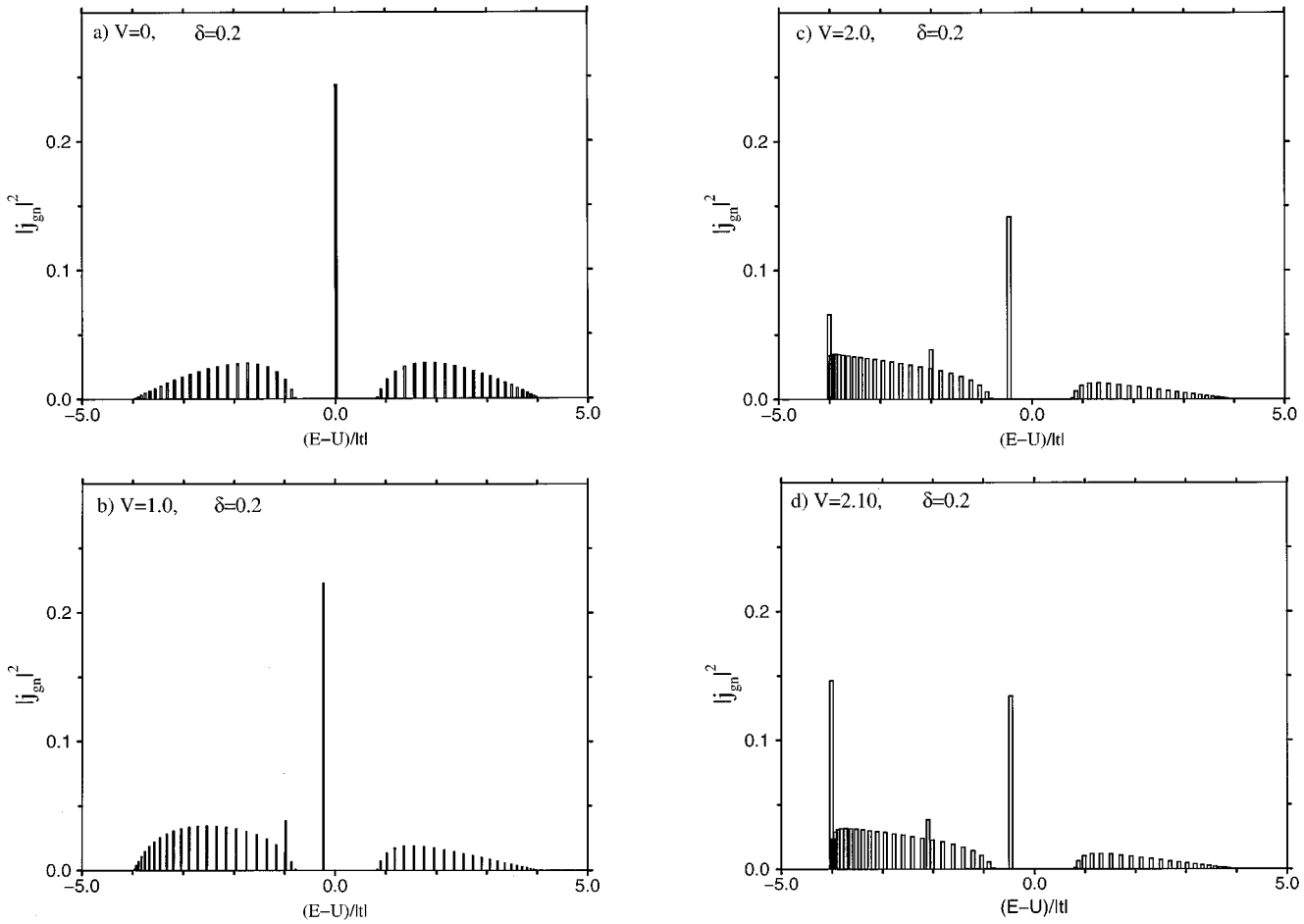

FIG. 5. The reduced optical conductivity for the dimerized extended Hubbard model with short-range intersite interaction, for (a) $V_1=0$, (b) $V_1=|t|$, (c) $V_1=2|t|$, (d) $V_1=2.1|t|$. The bond alternation parameter is δ in all cases. Note the excitons at $U-V_1$ and at $\leqslant U$, absent in Fig. 2. The lowest exciton now gains oscillator strength with increasing V_1 at the expense of the band center exciton at $\leqslant U$.

dominantly on the long bond for large dimerization, a result that we have confirmed from exact short chain calculations to be true also for intermediate U.[19] While the intermediate energy exciton is predominantly located on the short bond, the band center exciton is predominantly located on the long bond again. Furthermore, the relative signs of the coefficients of the basis functions containing the neighboring particle-hole pair are the same for the $K=0$ exciton and the band center exciton, thereby indicating that these two excitons occur in the same symmetry subspace even when the C_N rotational symmetry is reduced to $C_{N/2}$ by dimerization, and explaining the strong interaction between them, as observed from the exchange of oscillator strength between them when V_1 is varied in our optical absorption calculations (see Fig. 5). The large increase in the coefficients for the band center exciton with increasing δ explains the large intensity of the optical absorption to this state for nonzero bond dimerization.

IV. LONG-RANGE INTERACTIONS

Although models with short-range Coulomb interactions are applicable to segregated stack charge-transfer solids,[47] strictly speaking they are inapplicable to π-conjugated polymers, which have traditionally been described within Pariser-Parr-Pople (PPP) models with long-range Coulomb

TABLE I. Configuration space description of the eigenstates of the three exciton states obtained within the dimerized extended Hubbard model with short-range intersite interaction $V_1/|t|=2.5$, for three different bond dimerization parameters. In increasing order of energy, the excitons are labeled as $K=0$, π, and U, respectively. The ''short'' and ''long'' refer to short and long bonds. The numbers against these are the normalized coefficients of basis functions with the particle and the hole localized on these bonds. These signs are the same for the $K=0$ exciton and the band center exciton labeled U, but opposite for the $K=\pi$ exciton. For large δ, the former are localized on the long bond, while the $K=\pi$ exciton is localized on the short bond. The energies are in units of $|t|$, and relative to U.

$V=2.50$	$\delta\cong 0(0.01)$	$\delta=0.20$	$\delta\cong 1(0.95)$
$K=0$ Short	+0.42	+0.34	+0.02
Long	+0.43	+0.51	+0.71
Energy	−4.10	−4.13	−4.84
$K=\pi$ Short	+0.71	+0.83	+0.99
Long	−0.70	−0.55	−0.02
Energy	−2.50	−2.50	−2.50
U Short	+0.093	+0.19	+0.02
Long	+0.094	+0.28	+0.61
Energy	−0.455	−0.515	−1.13

interactions.[28] It is here that the advantage of the transformation to the spin Hamiltonian becomes obvious. In the present section we discuss the results of our calculations for the case of long-range intersite interaction. Both similarities and differences with the nearest-neighbor intersite interaction case are found.

Exact solutions are not available for the spin Hamiltonian with long-range z-z interaction even for $\delta=0$. On the other hand, numerical calculations of the states with two reversed spins as well as the coupling between these excited states and the ferromagnetic ground state still remain simple. Several different complications arise now, however, of which the most important are the following. First, as we show below, for long-range interactions there occur multiple $K=0$ excitons even for $\delta=0$, and the exciton binding energy is no longer the energy difference between the lowest two eigenstates even for this simple case. The very identification of eigenstates as excitonic or bandlike is therefore more difficult than before. Secondly, for weak long-range interactions, the lowest exciton is weakly bound and of Wannier nature (see below), and determination of its exciton character requires that the numerical calculations be performed for very long ring sizes.

In our numerical approach, we identify excitons and continuum states from the calculated optical absorption spectra and a spin-spin correlation function that is equivalent to the particle-hole correlation function within the electron model. As seen from the optical absorption spectra in Figs. 2 and 5, absorption to the exciton states is always larger than to the neighboring band states. Thus the relative strengths of the absorptions to neighboring states give one means of identifying exciton versus band states. Additional confirmation of exciton versus continuum character of a given eigenstate can be obtained from the numerically evaluated correlation function

$$d_{ij}=\langle (S_i^z+1/2)(S_j^z+1/2)\rangle \tag{12}$$

as a function of the separation $|i-j|$ within H_s. In the above, d_{ij} gives the radius of the bound two-magnon, or the exciton radius for the fermion case. As shown below, these two complementary procedures yield identical results in all cases.

Case A: $\delta=0$. We have assumed a $1/r$ form for the long-range Coulomb interaction, viz., $V_j=V_1/j$. The numerical calculations were performed for many different $V_1/|t|$, as one of our goals is to determine whether or not there exists a critical value of V_1 for the $K=0$ exciton to appear when the potential is of the $1/r$ form. As mentioned above, identification of the exciton states from numerical calculations require larger and larger ring sizes as V_1 is reduced. For the smallest V_1, the calculations were done for rings containing 500 atoms.

In Figs. 6(a)–6(c) we show plots of $|j_{gn}|^2$ for $\delta=0$ and $V_1=0.5$, 1.0, and 2.0, respectively. The insets show the region immediately about the absorption edge, magnified. From the inset of Fig. 6(a), the absorption to the lowest state is stronger than that to the second state, identifying the former as an exciton. Similarly, there occur two and three excitons, respectively, for $V_1/|t|=1.0$ and 2.0. An interesting observation is that in all cases the electron-hole continuum edge continues to be at $U-4|t|$, and its width remains $8|t|$. Further increase in V_1 creates additional excitons, and transfers more of the oscillator strength to the exciton states from the continuum states. The relative oscillator strengths of the transitions to the exciton states decrease with their energies.

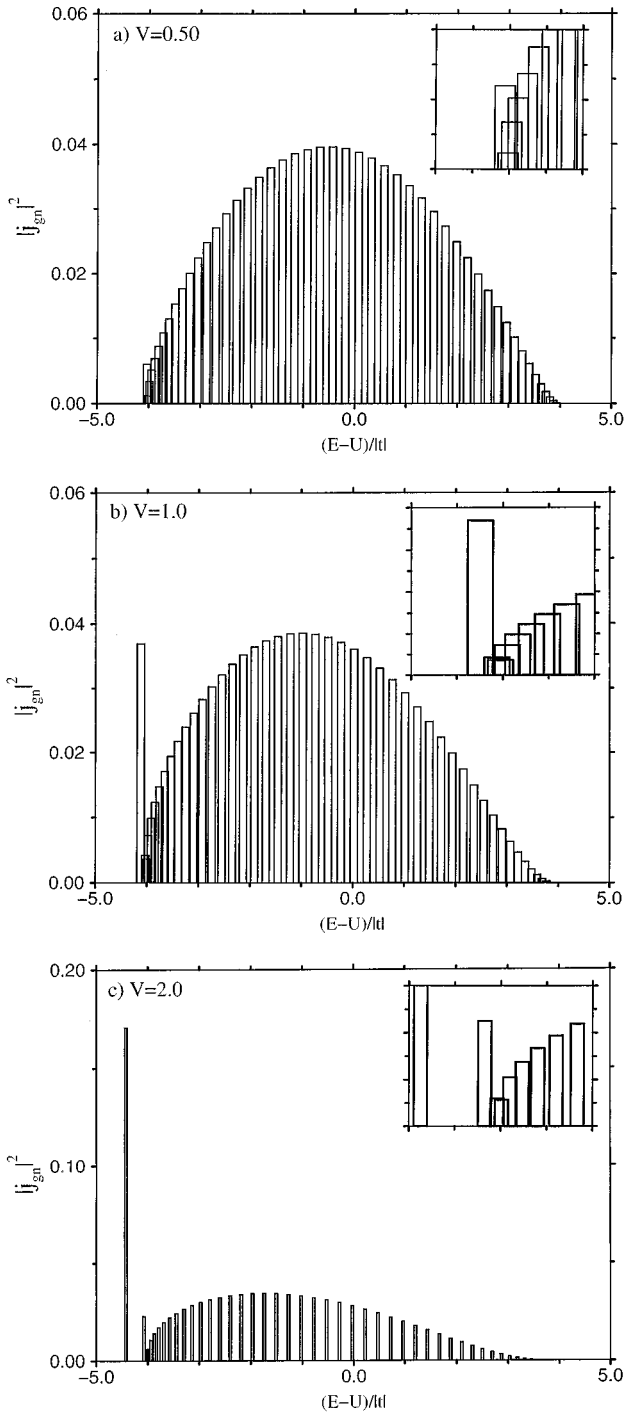

FIG. 6. The reduced optical conductivity for the undimerized extended Hubbard model with long range $V_j=V_1/j$, for (a) $V_1=0.5|t|$, (b) $V_1=|t|$, (c) $V_1=2.0|t|$. The vertical bars again correspond to individual $|j_{gn}|^2$, centered at the energy of the excited state n. The insets show the absorptions at the lower-energy threshold, magnified. From the insets, one, two and three distinct excitons occur in (a), (b), and (c), respectively (see text).

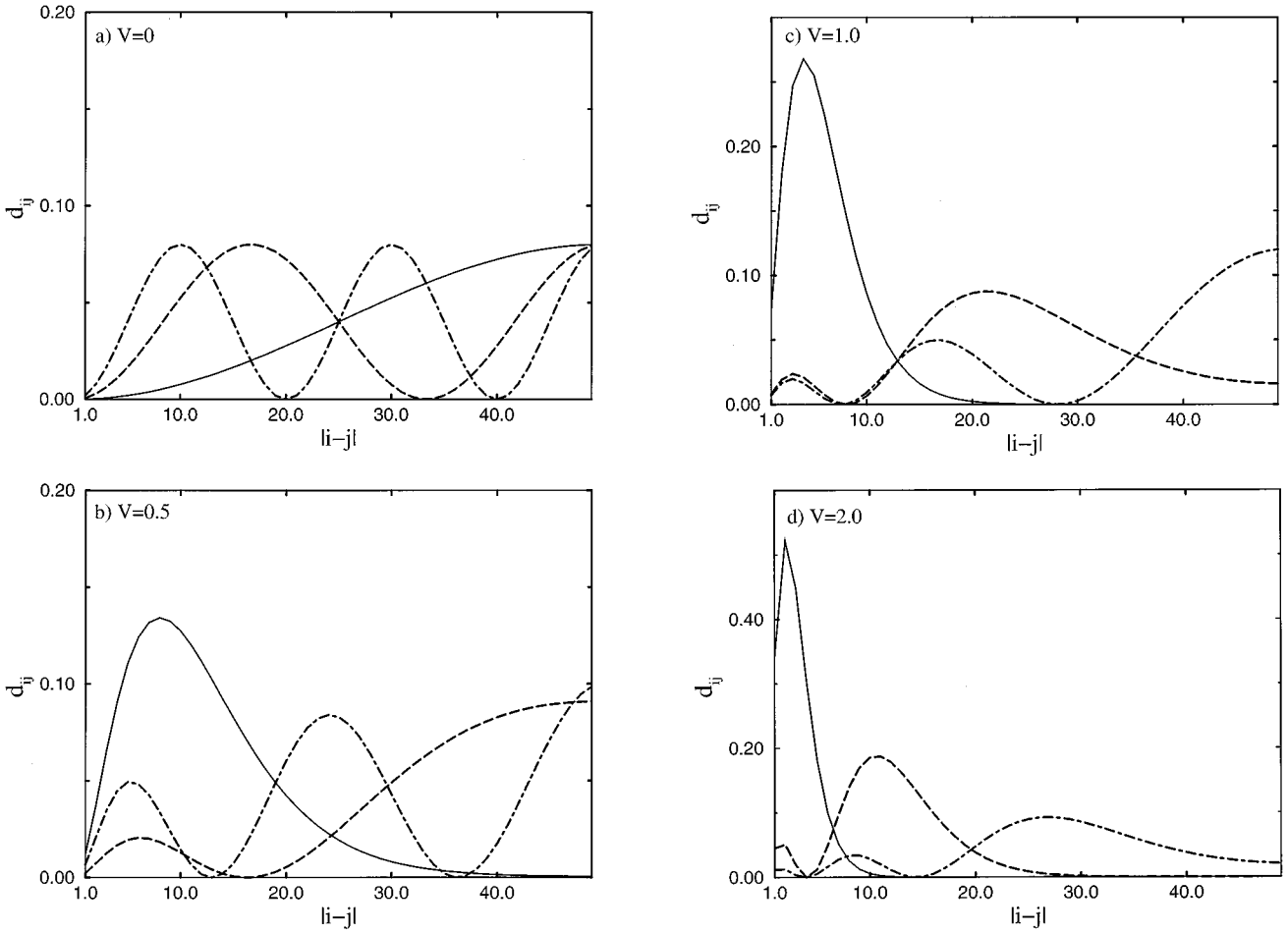

FIG. 7. The particle-hole correlations d_{ij} in the lowest three eigenstates in the undimerized extended Hubbard model with $V_j = V_1/j$, for (a) $V_1 = 0$, (b) $V_1 = 0.5|t|$, (c) $V_1 = |t|$, (d) $V_1 = 2.0|t|$. The solid, dashed, and dashed-dotted curves correspond to the lowest, the second, and the third eigenstate, respectively. No bound state occurs in (a), while one, two, and three bound states occur in (b), (c), and (d), respectively, in agreement with the results of Fig. 6. The exciton radius in the lowest exciton decreases progressively with increasing V_1.

The correlation functions d_{ij} corresponding to these parameters are shown in Fig. 7, where in Fig. 7(a) we have also included the d_{ij} behavior for the case of $V_1 = 0$. Although there occur nodes in d_{ij} for the higher-energy states for $V_1 = 0$, the continuum character of all eigenstates is obvious for this case from the delocalized nature of d_{ij}. In contrast, in Fig. 7(b), the lowest state has acquired localized character, with considerably smaller particle-hole separation. The particle-hole correlations for the second and third eigenstates are larger at larger separations, indicating these eigenstates to be delocalized again. These conclusions are in agreement with our conclusions obtained from the examination of the optical absorption spectrum in Fig. 6(a). Similarly in Figs. 7(c) and 7(d) we see that now the lowest two and three states are bound. As is expected, the particle-hole separation in the lowest exciton decreases progressively as V_1 is increased.

We have calculated both the optical absorption and the correlation function d_{ij} for chains of up to 500 atoms to determine whether or not there exists a critical strength of V_1 for exciton formation at $K = 0$. In Fig. 8(a) we have shown the optical absorption near the absorption edge for $V_1 = 0.065|t|$. The corresponding particle-hole correlation function behavior for the lowest eigenstate is shown in Fig. 8(b). Both results indicate the bound character of the lowest $N_2 = 1$ eigenstate, although the exciton radius is now very large. We conclude that the critical strength of V_1 vanishes asymptotically for $N \to \infty$.

In the above, we have focused only on the $K = 0$ sector of the energy spectrum. In Fig. 9 we have shown the numerically calculated complete energy spectrum for the $1/r$ potential for the case of $V_1 = 2|t|$. Three distinct exciton states are found with such a large V_1. The effective masses of the excitons increase with their energies.

Case B: $\delta \neq$. As in Fig. 3, dimerization reduces the size of the Brillouin zone. The optical absorption spectrum for $V_1 = 2|t|$ and $\delta = 0.2$ is shown in Fig. 10, where excitons again occur in pairs, one member of the pair occurring at low energy near the absorption edge, with the other member occurring deep inside. In addition, the band center exciton continues to be visible. The binding energies of the lowest $K = 0$ exciton, for different δ, are plotted against V_1 in Fig. 11. Here all calculations for the smallest V_1 were performed for periodic rings of 500 sites. As in the case of nearest-neighbor interaction, the dependence on δ of the binding energy is quantitative only, and weak. Note, however, that the absolute binding energies of the exciton in the present case of long range intersite interaction are considerably larger than those in Fig. 4 for the same V_1.

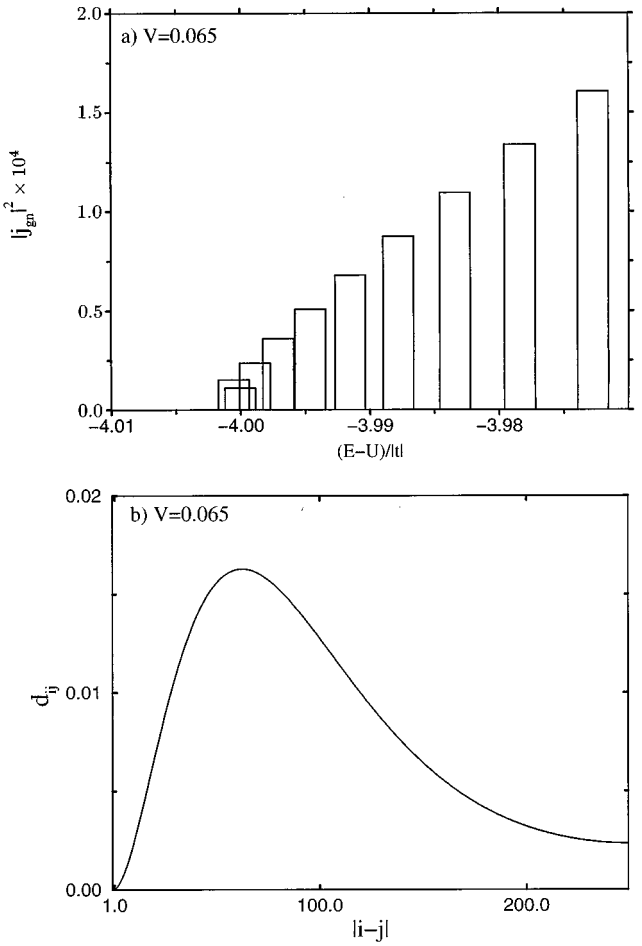

FIG. 8. The reduced optical conductivity for the undimerized extended Hubbard model with $V_j = V_1/j$, for $V_1 = 0.065|t|$. Note the expanded scale on the energy axis. (b) The particle-hole correlation d_{ij} in the lowest eigenstate for the same parameter. The lowest eigenstate is an exciton from both (a) and (b).

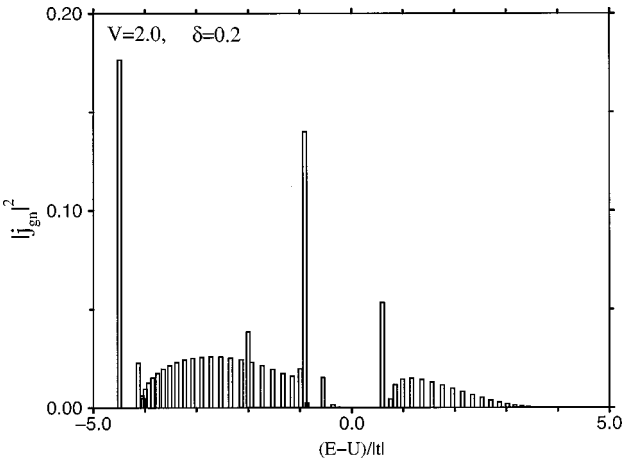

FIG. 10. The reduced optical conductivity for the dimerized extended Hubbard model with $V_j = V_1/j$, for $V_1 = 2.0|t|$. Two exciton states corresponding to each exciton in Fig. 6 are optically visible. In addition, the band center exciton is also visible, as in Fig. 5.

V. DISCUSSIONS AND CONCLUSIONS

In summary, we have shown that the $N_2 = 1$ subspace of $U \gg |t|$ extended Hubbard models can be mapped exactly into the sector of two reversed spins for the Ising-Heisenberg ferromagnetic chain. For the case of intersite Coulomb interactions zero beyond V_1, exact solution for the spin chain shows that at $K = 0$, the exciton appears only for $V_1 > 2|t|$. The critical strength of V_1 and the exciton binding energy change weakly for realistic nonzero dimerization δ, and only for $\delta \geq 0.5$ are the two quantities substantially different. Optical absorption spectra are dramatically different for zero and nonzero δ, and the difference can be understood within the context of simple folding of the exciton and the electron-hole continuum bands. For the $1/r$ potential, the lowest $N_2 = 1$ state is always an exciton irrespective of the value of V_1, while for $V_1 \geq |t|$ onwards multiple excitons begin to appear. Optical absorption is strongest to the lowest exciton. The effective masses of the excitons increase with increasing energy. The qualitative change in the absorption spectra

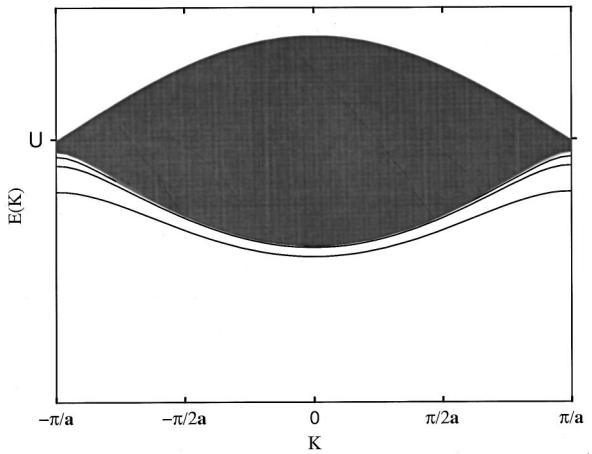

FIG. 9. The energy spectrum of the $N_2 = 1$ subspace of the undimerized extended Hubbard Hamiltonian with $V_j = V_1/j$, for $V_1 = 2|t|$. Three distinct exciton states (solid lines) are seen [see also Figs. 6(c) and 7(d)].

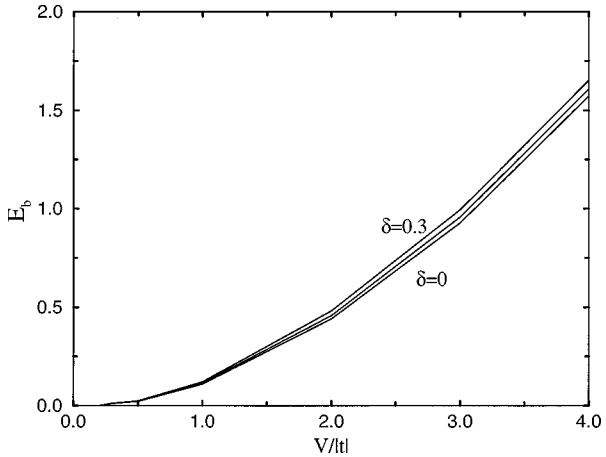

FIG. 11. The binding energy of the lowest $K = 0$ exciton, in units of $|t|$, as a function of $V_1/|t|$ for long range Coulomb interaction V_j/j. The central curve corresponds to $\delta = 0.2$. Note that the scale of energy is much larger than that in Fig. 4.

upon dimerization are similar to that in the short-range interaction case.

The most direct application of the present theory is to the half-filled band charge-transfer solids potassium tetracyanoquinodimethane (K-TCNQ) and rubidium tetracyanoquinodimethane (Rb-TCNQ). In these systems each alkali metal donates an electron to a TCNQ molecule, and the hopping of electrons between the weakly overlapping π-molecular orbitals of the $TCNQ^-$ anions lead to charge-transfer bands in the infrared. It is generally accepted that the repulsive interactions between two electrons in a $TCNQ^{2-}$ dianion is large compared to the one-electron bandwidth and that the condition $U \gg |t|$ is applicable. Furthermore, because of the large intermolecular separations, interactions beyond V_1 are negligible.[47] Half-filled band systems are known to undergo the spin-Peierls dimerization at low temperature, and in both K-TCNQ and Rb-TCNQ the spin-Peierls transition has been observed[48,49] (below 395 and 381 K, respectively). From polarized reflectance spectra of the crystals, it was shown by Yakushi *et al.*[50,51] that in both cases at low temperatures two distinct absorption bands are observed, a low-energy strong band with a peak at 1.1 eV and a high-energy shoulder at 1.4–1.5 eV. Yakushi *et al.*[50,51] and Mazumdar and Soos[52] had attributed the low-energy band to absorption to a charge-transfer exciton (consisting of nearest neighbor $TCNQ^{2-}$ and $TCNQ^0$) at energy $U-V_1$ and the high-energy band to absorption to the electron-hole continuum, which, however, was assumed to be at U instead of the $U-4|t|$ found here. Later experimental work by Okamoto *et al.*[53] demonstrated quite definitively that the high-energy absorption occurs only in the dimerized state. A similar conclusion was also reached by Meneghetti,[54] based upon direct numerical calculation of the optical absorption spectrum of a dimerized periodic ring of four sites. Our results in Fig. 5, however, indicate that dimerization makes two different high-energy excitons optically visible (because of strong finite-size effects, the four-site dimerized periodic ring has only one of these exciton states optically visible). We note that if the high-energy absorption at 1.5 eV in the CT solids[50,51,53] is assigned to the nominally $K=\pi$ exciton at $U-V_1$, Fig. 5 would predict an even higher-energy absorption at $\leqslant U$. No such absorption is seen in the real materials, even though in K-TCNQ in particular the reflection spectra go up to 2.0 eV. Based on the above experimental observations and the relative oscillator strengths of the $K=\pi$ exciton and the band center exciton in Fig. 5, we therefore assign the high-energy CT absorption to the band center exciton at $\leqslant U$. This would require $U-V_1-4|t|^2/V_1=1.1$ eV, $U \sim 1.5$ eV, yielding a modest $V_1 \sim 0.2$ eV for $|t| \sim 0.1$ eV, in agreement with most other estimates of these parameters, based on different experiments.[47]

Direct applications to π-conjugated polymers is more difficult. Within the standard PPP models[28] $U \sim 4|t|$, and the large-U approximation is not strictly appropriate. On the other hand, the very large value of V_1 within the standard models ($\sim 2-3|t|$), when taken together with the present result that the critical strength of V_1 for the formation of the $K=0$ exciton approaches zero for long-range V_j, indicates that the lowest optical absorption is to an exciton in π-conjugated polymers. The very large values of the binding energies of the lowest exciton in Fig. 11, when compared to those in Fig. 4, further indicate that while the qualitative features of PPP models can be obtained within the extended Hubbard model with short-range intersite interaction, the quantitative behavior are very different.

The strongest effect of finite U on the exciton states would be to create an energy splitting $2|t|^2/(U-V_1)$ among the degenerate odd and even parity excitons, due to nonzero H_3. While this reduces the energy of the odd parity exciton (which occurs below the even parity exciton[14]), we speculate that the energy of the lower threshold of the electron-hole continuum is reduced more due to greater delocalization at finite U. The latter behavior would be expected, for instance, from the behavior of the optical gap of the undimerized Hubbard model as a function of U, where it is known that the gap increases very slowly with U for $U<4|t|$, and only for still larger U is there a rapid increase. Thus for the same V_j, we anticipate smaller exciton binding energies for realistic U. On the other hand, since the exciton behavior is determined primarily by intersite Coulomb interactions, we believe that the weak dependence of the exciton binding energy on the dimerization parameter δ found here remains valid even for moderate U. Physically, a strong δ dependence in linear chains (for $\delta \leqslant 0.3$) is unexpected. We speculate that the observed differences in exciton binding energies between different π-conjugated polymers are either due to a large difference in V_1 (for example, compared to the polyacetylenes, the triple bond in the polyacetylenes has a very short length of only 1.2 Å, which would lead to larger V_1) or due to different connectivities (for example, in the poly-paraphenylenes and poly-paraphenylenevinylenes, each para carbon atom of a phenyl ring interacts with three neighbors, in contrast to only two in the linear chain systems). Unfortunately, the present calculations cannot be extended to systems containing aromatic ring systems, as the Jordan-Wigner transformation is invalid with such a boundary condition. It is, however, interesting to note that recent DMRG calculations for poly-paraphenylenevinylene,[55] which takes into account the actual structure of the material instead of replacing it with a linear chain,[27] finds an exciton binding energy of 1.2 eV. A similar value has also been reached by Barford and Bursill within a somewhat modified DMRG scheme that also retains the connectivity of poly-paraphenylenevinylene.[56]

The present calculations can be easily extended to study biexcitons and two-exciton continuaa in the large U limit. These eigenstates are in the $N_2=2$ sector of extended Hubbard models, Jordan-Wigner transformation of which leads to the four reversed spin sector of the Ising-Heisenberg spin chain.[38] Benchmark applications to nonlinear exciton-to-biexciton absorptions are anticipated. It has been claimed that such exciton to biexciton photoinduced absorptions are relevant in ultrafast photophysics of π-conjugated polymers.[11] With some modifications, it should be also possible to discuss the biexciton states in mixed-stack charge-transfer solids[22] within the same technique. These results will be discussed elsewhere.[38]

ACKNOWLEDGMENTS

S.M. acknowledges valuable discussions with Tom Kennedy and Stephan Koch and stimulating correspondence with Florian Gebhard. The numerical data for Fig. 13 were

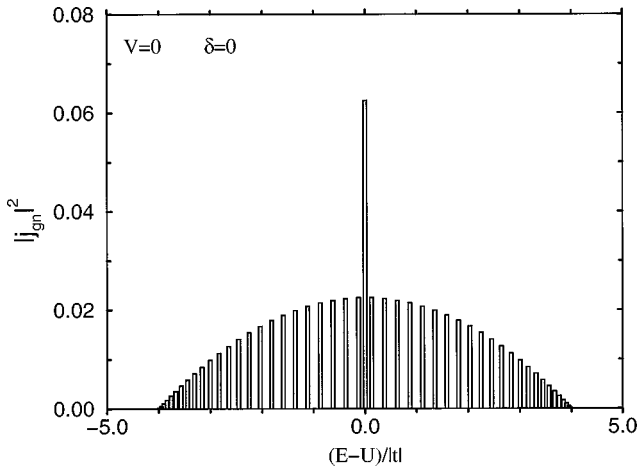

FIG. 12. The reduced optical conductivity for the undimerized simple Hubbard Hamiltonian, where the initial state is the dimer ground state [Eq. (A1), see text].

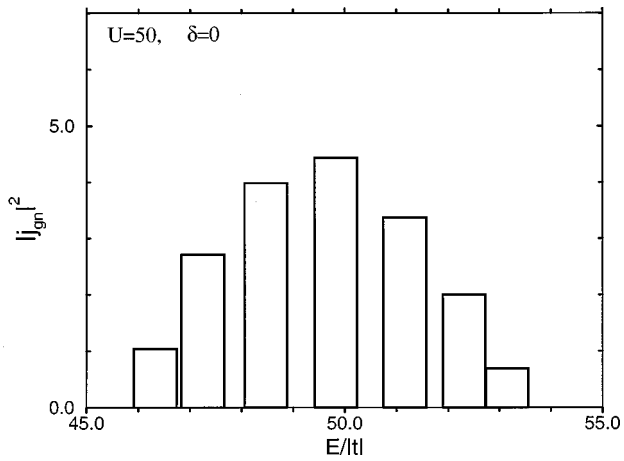

FIG. 13. The exact reduced optical conductivity for an undimerized open chain of 8 atoms, with $U/=50|t|$, $V_j=0$, $\delta=0$.

obtained by Yukihiro Shimoi (Electrotechnical Laboratory, Japan). We acknowledge support from the NSF (Grant No. ECS-9712171), the AFOSR, and the ONR through the MURI center (CAMP) at the University of Arizona.

APPENDIX

As mentioned in Sec. III, Gebhard *et al.* have presented a partial discussion of the consequences on the optical absorption of choosing a ground state that is different from the strictly AF state.[32] Specifically, long-range antiferromagnetic order does not occur in one dimension for any value of U, and even in the absence of true spin-Peierls dimerization nearest-neighbor spins are singlet coupled. Gebhard *et al.* therefore chose the perfect spin singlet dimer state

$$\psi_l=\Pi_i 2^{-1/2}(c^\dagger_{2i-1,\uparrow}c^\dagger_{2i,\downarrow}-c^\dagger_{2i-1,\downarrow}c^\dagger_{2i,\uparrow})|0\rangle \qquad \text{(A1)}$$

and calculated the absorption from this particular state to the $N_2=1$ subspace to determine the effects of singlet spin correlation [here $|0\rangle$ is the vacuum]. Within the authors' formalism, the calculation of the absorption from this state again requires formidable algebra, specifically because of the spin correlations. Within our approach the calculation of the optical absorption from the above dimer state is still simple. We note that even in the dimer state there is no effect of excited-state spin correlation on the optical absorption, since the matrix elements of charge exchange between a double occupancy and a singly occupied site, or that between a vacancy and a singly occupied site, is independent of spin within the $N_2=1$ subspace. The optical absorption from the dimer state is affected only by the spin correlations in the dimer ground state ψ_l, in which the probability that nearest-neighbor electron pairs have opposite spins is exactly 1 for the spin-bonded sites $2i-1$ and $2i$ but only 1/2 for the nonbonded sites $2i$ and $2i+1$. Within the Hamiltonian of Eq. (2) for $H_3=0$, this difference between bonded and nonbonded pairs of sites would be reflected in the matrix elements of $\hat{j}$ [Eq. 6], since the matrix element of $c^\dagger_{2i,\sigma}c_{2i+1,\sigma}$ is exactly one-half of the matrix element of $c^\dagger_{2i-1,\sigma}c_{2i,\sigma}$. Within the spin Hamiltonian H_s, j_{gn} is therefore given by $\Sigma_i[t_{2i-1}\langle g|S^\dagger_{2i-1}S^\dagger_{2i}|n\rangle+(1/2)t_{2i}\langle g|S^\dagger_{2i}S^\dagger_{2i+1}|n\rangle]$. Our calculated optical absorption within H_s with the above expression for j_{gn} is shown in Fig. 12 for $V_j=0$ and $\delta=0$. The calculated absorption spectrum shows a peak at U, as in the case of the dimerized AF ground state [see Fig. 5(a)], but does not have a gap in the density of states (since $\delta=0$ here). The spectrum in Fig. 12 is identical to that obtained by Gebhard *et al.* (see Fig. 1 in Ref. 32).

From the absorption spectrum for the dimer state Gebhard *et al.* conclude that the peak at energy U should be generic to the absorption within extended Hubbard models and the absorption from the AF ground state is a special case [Fig. 2(a)]. This, however, is not true in the absence of actual spin-Peierls dimerization, in spite of singlet spin correlations in one dimension. This is because in the absence of spin-Peierls dimerization, the ground state has equal contributions from ψ_l above and from ψ_r, defined as

$$\psi_r=\Pi_i 2^{-1/2}(c^\dagger_{2i,\uparrow}c^\dagger_{2i+1,\downarrow}-c^\dagger_{2i,\downarrow}c^\dagger_{2i+1,\uparrow})|0\rangle, \qquad \text{(A2)}$$

where now singlet spin couplings are between a different pair of neighbors. For equal contributions by ψ_l and ψ_r to the ground-state wave function, the same relative weights for the matrix elements of $S^\dagger_{2i-1}S^\dagger_{2i}$ and $S^\dagger_{2i}S^\dagger_{2i+1}$ are implied for optical absorption within H_s, so that the peak at U is lost.

Whether or not the true ground state is closer to ψ_l alone (or ψ_r alone), as opposed to an equal admixture of the two, can then be determined by exact calculation of the optical absorption within the Hamiltonian of Eq. (2). Since the latter can be done only for finite systems, understanding the effects of boundary conditions and chain lengths become important. In small periodic rings with an equal number of odd and even bonds, the ground state necessarily has equal contributions from ψ_l and ψ_r.[2] This is precisely why the optical absorption, as calculated by Loh and Campbell[42] for a periodic ring of 12 atoms within the simple Hubbard model resembles the absorption spectrum of Fig. 2(a). In open chains, the contributions by ψ_l and ψ_r are unequal, as ψ_r possesses one nearest-neighbor singlet bond less than ψ_l. Since the difference in the number of singlet bonds between ψ_l and ψ_r is 1 independent of chain length, the shorter the open chain, the stronger is the difference between the contributions by ψ_l and ψ_r to the true ground state. The difference therefore decreases as $1/N$, where N is the chain length. Thus any

tendency for the peak at U would be the strongest in the shortest open chains. In Fig. 13 we show the exact optical absorption for an open chain of 8 atoms for $U=50|t|$ and $\delta=0$. As in the calculation of Loh and Campbell, no signature of a peak at U is seen, and the calculated absorption is very similar to that in Fig. 2(a), confirming that the true ground state is a nearly equal admixture of ψ_l and ψ_r even in this small system. We therefore conclude that the optical absorption from the AF ground state, and not from the dimer ground state of Eq. (A1), is representative of the absorption from the true ground state.

Of course, for nonzero δ, the absorption from the true ground state and from the dimerized AF state are similar, and the above distinction becomes meaningless. This may be seen in Fig. 2 of Ref. 32.

[1] A. J. Heeger, S. Kivelson, J. R. Schrieffer, and W.-P. Su, Rev. Mod. Phys. **60**, 781 (1988).

[2] D. Baeriswyl, D. K. Campbell, and S. Mazumdar, in *Conjugated Conducting Polymers*, edited by H. Kiess (Springer-Verlag, Heidelberg, 1992), pp. 7–133.

[3] See, for instance, *Polydiacetylenes*, edited by D. Bloor and R. R. Chance, Vol. 102 of *NATO Advanced Studies Institute Series E: Applied Sciences* (Martinus Nijhoff, Dordrecht, 1985).

[4] See, for instance, *Optical Probes of Conjugated Polymers and Fullerenes*, edited by Z. V. Vardeny and L. J. Rothberg [Mol. Cryst. Liq. Cryst. Sci. Technol., Sect. A **256** (1994)]. See also, Primary Photoexcitations in Conjugated Polymers, edited by N. Serdar Sariciftci (World Scientific, Singapore, in press).

[5] N. Tessler, G. J. Denton, and R. H. Friend, Nature (London) **382**, 695 (1996).

[6] F. Hide *et al.*, Science **273**, 1833 (1996).

[7] S. V. Frolov, W. Gellermann, M. Ozaki, K. Yoshino, and Z. V. Vardeny, Phys. Rev. Lett. **78**, 729 (1997).

[8] D. Guo, S. Mazumdar, S. N. Dixit, F. Kajzar, F. Jarka, Y. Kawabe, and N. Peyghambarian, Phys. Rev. B **48**, 1433 (1993).

[9] S. Abe, M. Schreiber, W. P. Su, and J. Yu, Phys. Rev. B **45**, 9432 (1992).

[10] P. C. M. McWilliams, G. W. Hayden, and Z. G. Soos, Phys. Rev. B **43**, 9777 (1991).

[11] J. M. Leng, S. Jeglinski, X. Wei, R. E. Benner, Z. V. Vardeny, F. Guo, and S. Mazumdar, Phys. Rev. Lett. **72**, 156 (1994).

[12] T. Kobayashi *et al.*, J. Opt. Soc. Am. B **7**, 1558 (1990).

[13] S. V. Frolov, W. Gellermann, Z. V. Vardeny, M. Ozaki, and K. Yoshino, Synth. Met. **84**, 493 (1997).

[14] F. Guo, M. Chandross, and S. Mazumdar, Phys. Rev. Lett. **74**, 2086 (1995).

[15] V. A. Shakin and S. Abe, Phys. Rev. B **50**, 4306 (1994).

[16] K. Ishida, H. Aoki, and T. Ogawa, Phys. Rev. B **52**, 8980 (1995).

[17] F. B. Gallagher and F. C. Spano, Phys. Rev. B **53**, 3790 (1996).

[18] Z. G. Yu, R. T. Fu, C. Q. Wu, X. Sun, and K. Nasu, Phys. Rev. B **52**, 4849 (1995).

[19] S. Mazumdar and M. Chandross, in Primary Photoexcitations in Conjugated Polymers, edited by N. Serdar Sariciftci (World Scientific, Singapore, in press).

[20] For an early reference, see Z. G. Soos, Annu. Rev. Phys. Chem. **25**, 121 (1974). For more recent references, see V. J. Emery, in *Low Dimensional Conductors and Superconductors*, edited by D. Jerome and L. G. Caron (Plenum, New York, 1987), pp. 47–60.

[21] See, for instance, *Organic Conductors*, edited by J. P. Farges (Marcel Dekker, New York, 1994).

[22] M. Kuwata Gonokami, N. Peyghambarian, K. Meissner, B. Fluegel, Y. Sato, K. Ema, R. Shimano, S. Mazumdar, F. Guo, T. Tokihiro, H. Ezaki, and E. Hanamura, Nature (London) **367**, 47 (1994).

[23] Y. Shimoi and S. Abe, Synth. Met. **78**, 219 (1996).

[24] J. Cornil, D. Beljonne, R. H. Friend, and J. L. Brédas, Chem. Phys. Lett. **223**, 82 (1994).

[25] M. Chandross, S. Mazumdar, M. Liess, P. A. Lane, Z. V. Vardeny, M. Hamaguchi, and K. Yoshino, Phys. Rev. B **55**, 1486 (1997); M. Chandross and S. Mazumdar, *ibid.* **55**, 1497 (1997).

[26] K. Ishida, H. Aoki, and T. Chikyu, Phys. Rev. B **47**, 7594 (1993).

[27] Z. Shuai, S. K. Pati, W. P. Su, J. L. Bredas, and S. Ramasesha, Phys. Rev. B **55**, 15 368 (1997).

[28] R. Pariser and R. G. Parr, J. Chem. Phys. **21**, 466 (1953); **21**, 767 (1953); J. A. Pople, Trans. Faraday Soc. **49**, 1375 (1953).

[29] S. K. Lyo and J. P. Gallinar, J. Phys. C **10**, 1693 (1977).

[30] S. K. Lyo, Phys. Rev. B **18**, 1854 (1978).

[31] F. Gebhard, K. Bott, M. Scheidler, P. Thomas, and S. W. Koch, Philos. Mag. B **75**, 13 (1997).

[32] F. Gebhard, K. Bott, M. Scheidler, P. Thomas, and S. W. Koch, Philos. Mag. B **75**, 47 (1997).

[33] Z. G. Yu, A. B. Saxena, and A. R. Bishop, Phys. Rev. B **56**, 3697 (1997).

[34] J. Hubbard, Proc. R. Soc. London, Ser. A **276**, 238 (1963).

[35] A. B. Harris and R. V. Lange, Phys. Rev. **157**, 295 (1967).

[36] P. W. Anderson, Phys. Rev. **115**, 2 (1959).

[37] D. J. Klein, Phys. Rev. B **8**, 3452 (1973).

[38] B. Starke and S. Mazumdar (unpublished).

[39] D. J. Klein and W. A. Seitz, Phys. Rev. B **10**, 3217 (1974). See also, J. Bernasconi, M. J. Rice, W. R. Schneider, and S. Strassler, *ibid.* **12**, 1090 (1975).

[40] P. F. Maldague, Phys. Rev. B **16**, 2437 (1977).

[41] S. Ramasesha and Z. G. Soos, J. Chem. Phys. **80**, 3278 (1994).

[42] E. Y. Loh., Jr. and D. K. Campbell, Synth. Met. **27**, A499 (1988).

[43] M. Wortis, Phys. Rev. **132**, 85 (1963). See also, D. C. Mattis, *The Theory of Magnetism*, Vol. I (Springer-Verlag, Berlin, 1988), pp. 147–156.

[44] E. H. Lieb and F. Y. Wu, Phys. Rev. Lett. **20**, 1445 (1968).

[45] S. Ramasesha, S. K. Pati, H. R. Krishnamurthy, Z. Shuai, and J. L. Bredas, Phys. Rev. B **54**, 7598 (1996).

[46] S. Mazumdar and D. K. Campbell, Phys. Rev. Lett. **55**, 2067 (1985).

[47] S. Mazumdar and A. N. Bloch, Phys. Rev. Lett. **50**, 207 (1983). S. Mazumdar and S. N. Dixit, Phys. Rev. B **34**, 3683 (1986); K. C. Ung, S. Mazumdar, and D. Toussaint, Phys. Rev. Lett. **73**, 2603 (1994).

[48] A. Hoekstra, T. Spoelder, and A. Vos, Acta Crystallogr., Sect. B: Struct. Crystallogr. Cryst. Chem. **28**, 14 (1972).

[49] M. Konno, T. Ishii, and Y. Saito, Acta Crystallogr., Sect. B: Struct. Crystallogr. Cryst. Chem. **33**, 763 (1977).

[50] K. Yakushi, T. Kusaka, and H. Kuroda, Chem. Phys. Lett. **68**, 139 (1979).
[51] K. Yakushi, S. Miyajima, T. Kusaka, and H. Kuroda, Chem. Phys. Lett. **114**, 168 (1985).
[52] S. Mazumdar and Z. G. Soos, Phys. Rev. B **23**, 2810 (1981).
[53] H. Okamoto, Y. Tokura, and T. Koda, Phys. Rev. B **36**, 3858 (1987).
[54] M. Meneghetti, Phys. Rev. B **44**, 8554 (1991).
[55] S. Ramasesha (private communications).
[56] W. Barford and R. J. Bursill, Chem. Phys. Lett. **268**, 535 (1997).